Available online at www.sciencedirect.com

ScienceDirect

Chinese Journal of Natural Medicines 2018, **16**(10): 0791–0800

Chinese Journal of Natural Medicines

Profiling and identification of chemical components of Shenshao Tablet and its absorbed components in rats by comprehensive HPLC/DAD/ESI-MS^n analysis

MIAO Wen-Juan[1, 3△], HU Ying[2△], JIA Li[2], ZHANG Chun-Xia[2], YANG Wen-Zhi[2, 3*], ZHANG Ping[1], GUO De-An[2, 3*]

[1] *Department of Pharmacy, Institute of Hematology and Blood Disease Hospital, Chinese Academy of Medical Sciences and Peking Union Medical College, Tianjin 300020, China;*

[2] *Tianjin State Key Laboratory of Modern Chinese Medicine, Tianjin University of Traditional Chinese Medicine, Tianjin 300193, China;*

[3] *State Key Laboratory of Natural and Biomimetic Drugs, School of Pharmaceutical Sciences, Peking University, Beijing 100191, China*

Available online 20 Oct., 2018

[ABSTRACT] Shenshao Tablet (SST), prepared from Paeoniae Radix Alba (PRA) and total ginsenoside of Ginseng Stems and Leaves (GSL), is a traditional Chinese medicine (TCM) preparation prescribed to treat coronary heart disease. However, its chemical composition and the components that can migrate into blood potentially exerting the therapeutic effects have rarely been elucidated. We developed an HPLC/DAD/ESI-MS^n approach aiming to comprehensively profile and identify both the chemical components of SST and its absorbed ingredients (and metabolites) in rat plasma and urine. Chromatographic separation was performed on an Agilent Eclipse XDB C_{18} column using acetonitrile/0.1% formic acid as the mobile phase. MS detection was conducted in both negative and positive ESI modes to yield more structure information. Comparison with reference compounds (t_R, MS^n), interpretation of the fragmentation pathways, and searching of in-house database, were utilized for more reliable structure elucidation. A total of 82 components, including 21 monoterpene glycosides, four galloyl glucoses, two phenols from PRA, and 55 ginsenosides from GSL, were identified or tentatively characterized from the 70% ethanolic extract of SST. Amongst them, seven and 24 prototype compounds could be detectable in the plasma and urine samples, respectively, after oral administration of an SST extract (4 g·kg^{-1}) in rats. No metabolites were observed in the rat samples. The findings of this work first unveiled the chemical complexity of SST and its absorbed components, which would be beneficial to understanding the therapeutic basis and quality control of SST.

[KEY WORDS] Shenshao Tablet; Paeoniae Radix Alba; Total ginsenoside of Ginseng Stems and Leaves; Chemical component

[CLC Number] R917 **[Document code]** A **[Article ID]** 2095-6975(2018)10-0791-10

Introduction

A major obstacle that hinders the globalization of traditional Chinese medicine (TCM) is the ambiguity of chemical composition (structures and contents) and the ingredients mainly responsible for the curative effects. Many efforts and strategies have been made to systematically identify what components are involved in TCM and which of them play the role of therapeutic basis [1-2]. Serum pharmacochemistry is a widely accepted vehicle that bridges the chemicals and pharmacology, and an initial task of this strategy is to clarify which of the chemicals can migrate into blood [3]. Currently, liquid chromatography/mass spectrometry-based approaches are the most acceptable solution to clarifying the multi-components of TCM and identifying the absorbed ingredients together with their metabolites in biosamples [4–8]. In particular, tandem mass spectrometry (MS/MS or MS^n) can offer the information of both precursors and multi-stage fragments,

[Received on] 18-May-2018

[Research funding] This work was financially supported by Tianjin Municipal Education Commission Research Project (No. 2017ZD07).

[*Corresponding author] Tel/Fax: 86-22-59596163, E-mail: ywz_0504@163.com (YANG Wen-Zhi); gda5958@163.com (GUO De-An)

△These two authors contributed to this work equally.

These authors have no conflict of interest to declare.

Published by Elsevier B.V. All rights reserved

which is orthogonal to retention time determined by LC, thus is in support of the rapid, sensitive identification of multi-components from herbal and biological matrices.

Shenshao Tablet (SST) is a reputable TCM formula used to treat coronary heart disease (CHD). It is prepared from Paeoniae Radix Alba (PRA; *Paeonia lactiflora* Pall.; Family Ranunculaceae) and total ginsenoside of Ginseng Stems and Leaves (GSL; *Panax ginseng* C.A. Mey.; Family Araliaceae) at a ratio of 1950 : 13. SST is able to lower the angina frequency and to improve the quality of life in CHD patients with stable angina pectoris [9]. A meta-analysis of the clinical randomized controlled trials also indicates the curative effects of SST for CHD are definite and safe [10]. In Chinese Pharmacopoeia (2015 edition), the contents of paeoniflorin ($C_{23}H_{28}O_{11}$), ginsenosides Rg_1 ($C_{42}H_{72}O_{14}$), Re ($C_{42}H_{82}O_{18}$), and Rd ($C_{42}H_{82}O_{18}$), are the quantitative assay markers to evaluate the quality of SST [11]. To the best of our knowledge, no reports are currently available for a systematic multicomponent characterization of SST and its absorbed components. However, accumulation of the knowledge regarding the chemical compositions of *Paeonia* and *Panax* genus, as well as two single species (PRA and GSL) has laid solid foundation to unveil the chemical compositions of SST. Previous phytochemical researches have isolated monoterpenes (and their glycosides), triterpenoids, flavonoids, phenols, tannins, and polysaccharides, *etc,* from *Paeonia* and PRA [12-13], and collision-induced dissociation (CID) of monoterpene glycosides, galloyl glucoses, and phenolic acids, has been extensively studied [14−19]. GSL contains abundant ginsenosides serving as the major bioactive ingredients, which can be classified into protopanaxadiol (PPD), protopanaxatriol (PPT), oleanolic acid (OA), C-17 side chain varied, and miscellaneous types based on structural difference of sapogenins [20−22]. The compositions of ginsenosides between GSL and *P. ginseng* root have been elucidated [23], and a library consisting of 646 ginsenosides identified from GSL has been established [24], which can greatly facilitate the characterization of ginsenosides from SST. By recurring to potent LC-MS analysis, the chemical components of SST and those migrating into blood can be rapidly and sensitively determined.

The aim of the current work was to develop an HPLC/DAD/ESI-MS^n approach to comprehensively profiling and characterizing the multi-components of SST and those in the plasma and urine of SST-administrated rats. Chromatographic and mass spectrometric conditions were optimized to enable the simultaneous fingerprinting analyses of SST and two component drugs. The fragmentation behaviors of 20 reference compounds in both negative and positive ESI modes were comparatively analyzed to aid the identification of those unknown components present in SST. Then the plasma and urine samples of rats after orally administrating an SST extract were collected and analyzed under the same conditions. The components present in biosamples were identified by comparison with those characterized from the SST extract. The findings obtained in the present study would be essential to deeply understand the mechanism of action for SST in treating CHD and simultaneously beneficial to its quality control.

Materials and Methods

Reagents and chemicals

Twenty compounds, including paeoniflorin (**1**: $C_{23}H_{28}O_{11}$), albiflorin (**2**: $C_{23}H_{28}O_{11}$), galloylpaeoniflorin (**3**: $C_{30}H_{32}O_{15}$), benzoylpaeoniflorin (**4**: $C_{30}H_{32}O_{12}$), lactiflorin (**5**: $C_{23}H_{26}O_{10}$), paeonivayin (**6**: $C_{30}H_{32}O_{12}$), paeoniflorin sulfonate (**7**: $C_{23}H_{28}O_{13}S$), isomaltpaeoniflorin (**8**: $C_{29}H_{38}O_{16}$), pentagalloyl glucose (**9**: $C_{41}H_{32}O_{26}$), gallic acid (**10**: $C_7H_6O_5$), ethyl gallate (**11**: $C_9H_{10}O_5$), ginsenosides Rb_1 (**12**: $C_{54}H_{92}O_{23}$), Rb_2 (**13**: $C_{53}H_{90}O_{22}$), Rb_3 (**14**: $C_{53}H_{90}O_{22}$), Rc (**15**: $C_{53}H_{90}O_{22}$), Rd (**16**: $C_{48}H_{82}O_{18}$), F_2 (**17**: $C_{42}H_{72}O_{13}$), 20(*S*)-Rg_3 (**18**: $C_{42}H_{72}O_{13}$), Re (**19**: $C_{48}H_{82}O_{18}$), and Rg_1 (**20**: $C_{42}H_{72}O_{14}$), isolated from the roots of *Paeonia lactiflora* [20] and *Panax ginseng* [21] by the authors, were used as the reference compounds. Their chemical structures are exhibited in Fig. 1. HPLC grade acetonitrile, methanol, and formic acid were from J.T Baker (Phillipsburg, NJ, USA), and ultra-pure water was prepared using a Milli-Q purification system (Millipore, Bedford, MA, USA). Shenshao Tablet (No. SST-20160301) was purchased from Tong Ren Tang Technologies Co. Ltd. (Beijing, China). The drug materials of PRA (PRA-20160201) and total ginsenoside of GSL (GSLTG- 20160401) were obtained from the local drugstores, and the voucher specimen were deposited at the authors' laboratory in Peking University.

Animals

Male Sprague-Dawley rats, weighing 250 ± 20 g, were obtained from Laboratory Animal Center of Peking University Health Science Center (Beijing, China). Animal Care and Use Committee of Peking University Health Science Center approved the animal facilities and protocols used all through this experiment. The rats were housed in animal room with the temperature varying 22−24 °C and relative humidity of 60%. The rats were fasted for 24 h prior to experiments, but free to taking deionized water.

Preparation of SST, PRA, and GSL samples for LC-MS^n analysis

The easy-to-implement ultrasonic extraction was utilized for preparing the test solutions of SST, PRA, and GSL extracts. Briefly, 200 mg of accurately weighed, pulverized powder was placed in a centrifuge tube (10 mL), with 2 mL of 70% aqueous methanol (*V*/*V*) being added. The sample was extracted on a water bath at 40 °C assisted with ultrasound for 30 min. The liquid was transferred into a tube and centrifuged at 14 000 r·min^{-1} for 10 min, with the obtained supernatant taken as the test solution (100 mg·mL^{-1}).

Preparation of SST extract for animal administration

The extract of SST was prepared by ultrasonically extracting 15 g of SST in 70% ethanol (300 mL) for 30 min. The extract after filtration was concentrated at 50 °C under reduced pressure to prepare a thick liquid without the alcohol flavor. It

was finally diluted to a constant volume at 45 mL to prepare the SST extract (333 mg·mL^{-1}) for animal experiments.

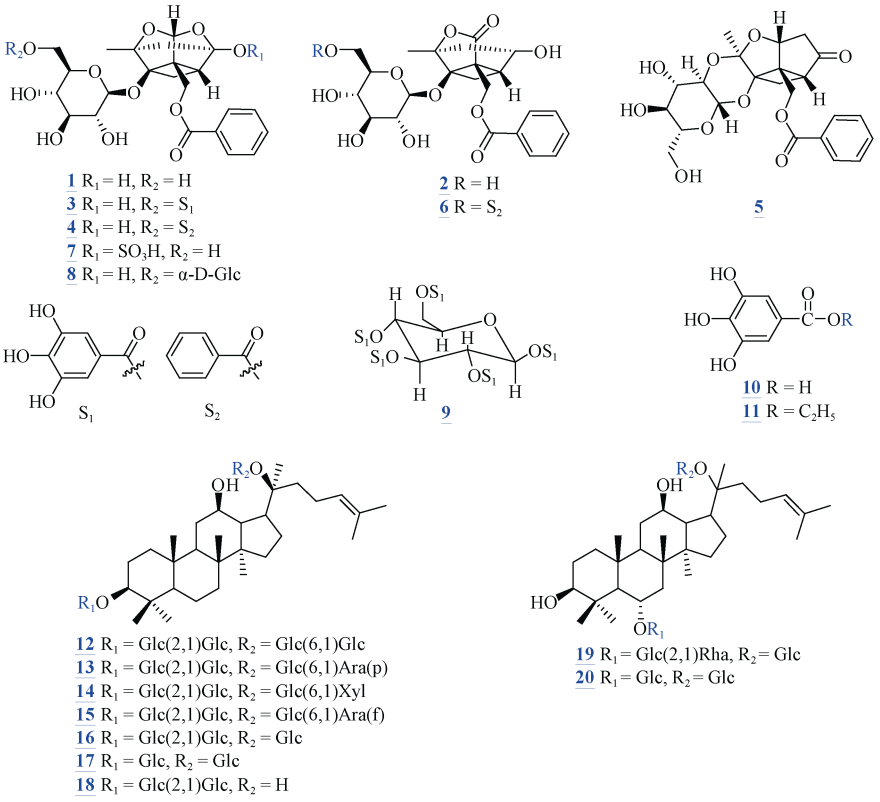

Fig. 1 Chemical structures of 20 reference compounds used in the present study

Preparation of rat plasma and urine samples

Fourteen male SD rats were divided into two groups: Control group (four) and SST group (ten). Control group was administrated with only saline, and every two rats were used to prepare the blank urine (0−24 h) and blank plasma samples. SST group were orally administrated with the SST extract (equal to 4 g·kg^{-1}). Two rats were housed in a metabolic cage for 24 h, and their urine was collected over 0–12 h and 12–24 h and finally combined. The blood was collected from femoral artery at 0. 5, 1.5, 4, and 12 h, after SST treatment, and was immediately centrifuged at 6000 r·min^{-1} (4 °C) for 20 min. The supernatant was separated and combined as the pooled plasma samples.

Each 500 μL of four SST-administrated samples collected at different timepoints were pooled (2 mL), and the obtained sample was further mixed with 6 mL of methanol, and vortexed for 5 min at 1500 r·min^{-1}. After centrifuge (9000 r·min^{-1}) for 20 min, the supernatant was collected and dried at a steady flow of nitrogen (N_2) at 40 °C. The resulting residue was reconstituted in 200 μL of 70% methanol. After being vortexed at 2000 r·min^{-1} for 3 min, the liquid was filtered through a 0.22-μm membrane.

Two mL of urine collected from the SST -administrated rats was loaded onto a pre-equilibrated SPE column. Successive elution by 5 mL of water, 5 mL of 5% methanol, and finally 5 mL of pure methanol was performed, and pure methanol eluent was dried under reduced pressure at 40 °C. The residue obtained was dissolved in 200 μL of 70% methanol. The liquid was filtered by use of the 0.22-μm membrane before analysis.

Chromatographic and mass spectrometry conditions

Chromatographic separation of all samples was performed using an Agilent 1100 series HPLC system (Agilent, Waldbronn, Germany) equipped with a quaternary pump, an autosampler, a column compartment, and a DAD detector. An Agilent Eclipse XDB C_{18} column (4.6 mm × 250 mm, 5 μm; Agilent Technologies, Santa Clara, CA, USA) hyphenated with a Zorbax SB C_{18} guard column was used at 35 ºC. A binary mobile phase consisting of 0.1% formic acid (A) and acetonitrile (B) ran at 1.0 mL·min^{-1} in accordance with the following gradient program: 0−7 min: 5%−18% (B); 7−16 min: 18%−25% (B); 16−19 min: 25%−30% (B); 19−45 min: 30%−38% (B); 45−50 min: 38%−45% (B); 50−55 min: 45%−90% (B); and 55−60 min: 90% (B). The DAD detector scanned over 190−400 nm. The injection volume was 10 μL.

Centroided MS^n data were recorded on a Finnigan LCQ Advantage 3D ion-trap mass spectrometer equipped with an ESI source operating in both negative and positive ESI modes (Thermo Finnigan, San Jose, CA, USA). Tune parameters were as follows: capillary temperature, 330 ºC; sheath gas (N_2),

40 arb; auxiliary gas (N_2), 10 arb; spray voltage: −4.5 kV (ESI−)/4.5 kV (ESI+); capillary voltage, −22 V/5 V; and tube lens offset, −60 V/50 V. In both negative and positive modes, the analyzer scanned over the mass range *m/z* 120–1200. Source fragmentation voltage of 25 V was enabled in the negative mode to suppress adduct precursors. Up to MS^4 data of the selected precursors (most abundant in each full-scan spectrum) by data-dependent collision-induced dissociation (CID) were recorded for structural elucidation, under normalized collision energy (NCE) of 32% for ESI^- and 34% for ESI^+, respectively.

Results and Discussion

The established HPLC/DAD/ESI-MS^n approach was utilized to comprehensively profile and identify the chemical components of SST. The multi-stage fragmentation behaviors of 20 reference compounds involving monoterpene glycosides, galloyl glucose, phenols, and ginsenosides (Fig. 1) in both negative and positive ESI modes were investigated to summarize useful neutral loss and diagnostic product ions supporting the characterization of unknown ingredients in SST. Both SST and two component drugs (PRA and GSL) were analyzed under the same condition to help identify those minor ingredients of the formula. Subsequently, the components absorbed by rats in the plasma and urine samples were elucidated by recurring to the chemical list of SST and MS^n analysis. Total ion chromatograms of PRA, GSL, SST, and the plasma and urine samples obtained in the negative ESI mode are exhibited in Fig. 2.

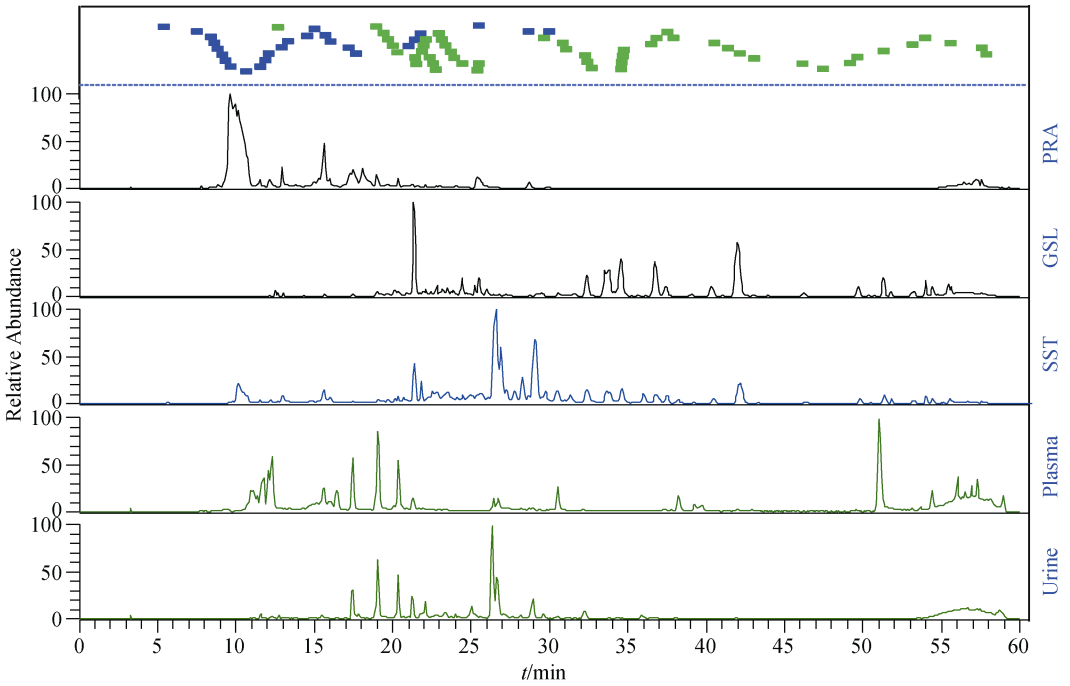

Fig. 2 Total ion chromatograms (TIC) of Paeoniae Radix Alba (PRA), Ginseng Stems and Leaves (GSL), Shenshao Tablet (SST), and SST-administrated plasma and urine samples of rats recorded in the negative ESI mode. The blue and green frames (topside) separately represent the components of SST characterized from PRA and GSL

Interpretation of the fragmentation pathways for 20 reference compounds

Monoterpene glycosides Monoterpene glycosides (MTG) with a cage-like pinane skeleton are the characteristic bioactive ingredients for medicinal *Paeonia* species [13, 25]. In negative ESI mode, eight MTG compounds could be readily ionized into the deprotonated precursors ($[M - H]^-$) and/or formic acid-adducts ($[M + HCOO]^-$). Typically, neutral elimination of CH_2O (30 Da) was observed for most of the studied MTGs (**1**−**4**, **6**, and **8**), with only **5** and **7** (a sulfite derivative) as the exceptions. This typical neutral elimination was speculated to occur at the hemiacetal structure of **1**, **3**, **4**, **8**, or C-5 of the glucose moiety for **2** and **6** [17]. Other neutral loss, such as benzoic acid (BZA; $C_7H_6O_2$, 122 Da), H_2O (18 Da), and Glc (162 Da), was common as well. In contrast, in the positive mode, ammonium-adduct ($[M + NH_4]^+$; **1**, **3**−**5**, **7**, and **8**) or protonated ($[M + H]^+$) molecules were detected being the base peaks. Notably, neutral elimination of CH_2O was not detected in the positive mode CID of MTGs. Additional neutral eliminations, including BZA (122 Da), Glc (162 Da) and Glc + H_2O (180 Da), were observed. The fragmentation pathways of galloylpaeoniflorin (**3**) were illustrated as an example (Fig. A.1). Its predominant precursors were observed at *m/z* 631 ($[M - H]^-$) and 650 ($[M + NH_4]^+$), respectively. The negative CID of *m/z* 631 generated MS^2 product ions at *m/z* 613 ($[M - H - H_2O]^-$), 601 ($[M - H - CH_2O]^-$), and 491 ($[M - H - H_2O - BZA]^-$), subsequent CID-MS^3 of *m/z* 613 yielded abundant fragments at *m/z* 491, 313 ([GalloylGlc −

H]$^-$), and 271. The product ions *m/z* 313 and 271 should be two separate component parts of a fragment obtained from *m/z* 613 after neutral elimination of CH_2O [16]. The positive CID of *m/z* 650 could easily lose NH_3 (17 Da) and suffer from diversified fragmentations producing MS^2 fragments at *m/z* 493 ([M + H − H_2O − BZA]$^+$), 475 ([M + H − $2H_2O$ − BZA]$^+$), and 315 ([GalloylGlc + H]$^+$, base peak). The CID-MS^3 product ions of *m/z* 315 included *m/z* 297 ([GalloylGlc + H − H_2O]$^+$), 285 ([GalloylGlc + H − CH_2O]$^+$), 171 ([GLA + H]$^+$), and 153 ([GLA + H − H_2O]$^+$). Notably, the positive CID behaviors of MTGs are rarely investigated in previous reports [14-15, 17-18, 25]. Additionally, due to the stove drying of PRA raw materials, MTG sulfites have been detected. As a representative, the fragmentation pathways of paeoniflorin sulfonate (**7**) are exhibited in Fig. 2. Typical fragmentation features involved the elimination of 46 Da (CH_2O_2) replacing the neutral elimination of 30 Da (CH_2O) in negative mode [15], and neutral loss of 82 Da (H_2SO_3) in positive mode. Key UV and MS information useful for characterizing SST components is indicated in Fig. 3.

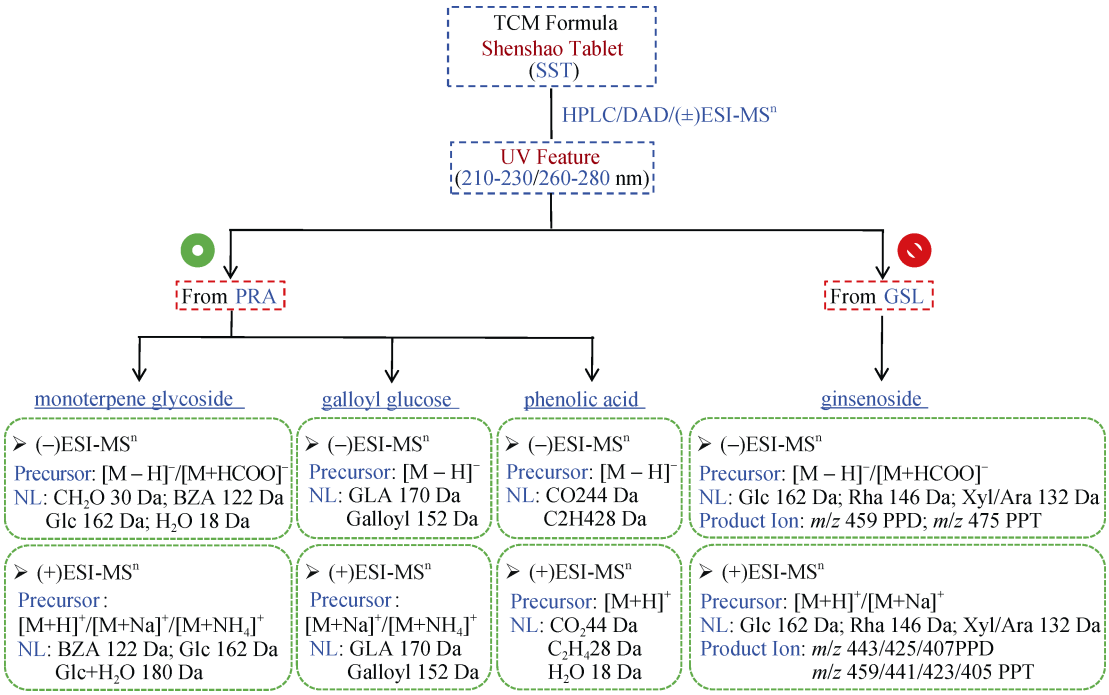

Fig. 3 Summary of the key UV and MS information useful for structural elucidation of SST components. PRA: Paeoniae Radix Alba; GSL: Ginseng Stems and Leaves; NL: neutral loss; BZA: benzoic acid; and GLA: gallic acid

Galloyl glucose

The only galloyl glucose reference compound pentagalloyl glucose (**9**) in structure was esterified with five galloyl substituents on the glucose skeleton. Predominant [M − H]$^-$ (*m/z* 939) and [M + NH_4]$^+$ (*m/z* 958) were the precursor ions in the negative and positive ESI modes, respectively. Successive eliminations of gallic acid (170 Da) and a galloyl substituent (152 Da) occurred by both the negative and positive CID-MS^4. In detail, the negative-mode precursor ion *m/z* 939 could be fragmented into the ions of *m/z* 787 ([M − H − Galloyl]$^-$), 769 ([M − H − GLA]$^-$; base peak), and 617 ([M − H − Galloyl − GLA]$^-$). Further fragmentation of the MS^2 base peak *m/z* 769 could obtain the fragments *m/z* 617, 599 ([M − H − 2GLA]$^-$), and 447 ([M − H − Galloyl − 2GLA]$^-$) [15, 18, 25]. Similar to MTGs, the [M + NH_4]$^+$ (*m/z* 958) precursors easily eliminated NH_3 and were fragmented into *m/z* 771 ([M + H − GLA]$^+$) as the base peak. Diverse CID-MS^3 product ions, including *m/z* 619 ([M + H − GLA − Galloyl]$^+$), 431 ([M + H − 3GLA]$^+$), 305 ([M + H − 3GLA − pyrogallol]$^+$), 279 ([M + H − 3GLA − Galloyl]$^+$), and 261 ([M + H − 4GLA]$^+$), were further dissociated from *m/z* 771. The fragmentation pathways in both negative and positive ESI modes are displayed in Fig. A.3.

Ginsenosides

Concomitant [M − H]$^-$ and formic acid-adduct [M + HCOO]$^-$ precursors rendering mass difference 46 Da in negative mode [24, 26−29], and the observation of [M + H]$^+$ and sodium-adduct [M + Na]$^+$ precursors together with in-source CID resulting product ion clusters in positive mode, are the "identity features" of ginsenosides [30−32]. CID behaviors of ginsenosides are typically characterized by successive neutral elimination of sugar residues to generate the product ions corresponding to the sapogenins (*m/z* 459 for PPD type and *m/z* 475 for PPT type) in negative mode. The neutrally eliminated masses by negative CID at 162 Da (reference compounds **12**−**20**, Fig. 1), 146 Da (**19**), and 132 Da (**13**−**15**), were consistent with the sugar residues Glc (hexose), Rha (methylpentose), Xyl/Ara (either in *pyran* or *furan* forms; pentose). In contrast, the positive-mode full-scan spectrum gave rich ion species, involving precursors

($[M + H]^+$/ $[M + Na]^+$), concomitant sugar- elimination product ions, and sapogenin-related ions at *m/z* 443/425/407 for PPD ginsenosides (**12**−**16**), and *m/z* 459/441/ 423/405 for PPT ginsenosides (**19** and **20**). The characteristic sapogenin ions, as the results of successive H_2O eliminations from the protonated precursors (*m/z* 443/425/407 for $[PPD + H - H_2O]^+$/$[PPD + H - 2H_2O]^+$/$[PPD + H - 3H_2O]^+$; *m/z* 459/441/423/ 405 for $[PPT + H - H_2O]^+$/$[PPT + H - 2H_2O]^+$/$[PPT + H - 3H_2O]^+$/ $[PPT + H - 4H_2O]^+$) should need further confirmation by high-resolution MS and comparison with pure sapogenin compounds, 20(*S*)-PPD and 20(*S*)-PPT [28−30]. As a typical case, the fragmentation pathways of ginsenoside F_2 (**17**) in the negative mode as well as the assignment of in-source CID products ions in positive mode are exhibited in Fig. A.4. Its precursor ions in negative mode were observed at *m/z* 829 (base peak) and 783. The CID-MS^2 fragments, *m/z* 621 and 459, were the results of successive neutral elimination of two Glc residues. In addition, the full-scan spectrum in positive ESI mode exhibited the precursors (*m/z* 807 for $[M + Na]^+$) and versatile IS-CID product ions, which included the protonated precursors after eliminating H_2O (*m/z* 767), Glc + H_2O (*m/z* 605), Glc + $2H_2O$ (*m/z* 587), Glc + $3H_2O$ (*m/z* 569), together with characteristic PPD sapogenin product ions at *m/z* 443, 425, and 407. Integrated analyses of the negative MS^n and positive full-scan data could offer much structural information that facilitate ginsenoside characterization.

Two phenol compounds (**10** and **11**) were efficiently ionized in the negative ESI mode, forming deprotonated precursors at *m/z* 169 and 197, respectively. Preferred neutral loss of CO_2 (44 Da) occurred for both two reference compounds, while the elimination of C_2H_4 (28 Da) was observed for **11** in the negative mode. Weak protonated precursor at *m/z* 199 occurred to **11**. Its CID-MS^2 exhibited the neutral eliminations of C_2H_4 and CO_2. Two minor product ions at *m/z* 109 and 81 resulted from successive cleavages of H_2O.

Based on the above analyses, an interpretation guideline diagram is presented in Fig. 3 to enable the characterization of multicomponents of SST based on the obtained HPLC/ DAD/ESI-MS^n data. In particular, useful neutral eliminations and diagnostic product ions are summarized.

Systematic profiling and identification of the multicomponents from SST

Under the current LC-MS condition, ginsenosides from GSL in general showed stronger retention than the components of PRA (Fig. 2), which may aid to characterize the multi-components of SST and assign their botanical source. The typical UV absorptions at 210−230 nm and 260−280 nm could be auxiliary in the primary characterization of benzoyl/galloyl MTGs and glucose from PRA [14-15]. To identify more components from SST, those minor failing to trigger the MS^n fragmentation but showing the same retention time (t_R) and *m/z* values (orthogonal information) in the extracted ion chromatograms (EIC) of SST and two single component herbs, were also considered. Their structural elucidation was performed mainly based on the MS^n data of two single herbs, searching of in-house libraries [24, 29], and comparison with literature [14−17, 21−29]. As a result of these efforts, a total of 82 components were identified or tentatively characterized from SST (Table 1), involving 27 (21 MTGs, four galloyl glucoses, and two phenols) from PRA and 55 ginsenosides from GSL. The detailed information with respect to all these characterized components from SST is given in Table A.1.

MTGs from SST. A total of 21 MTG components, showing a retention time in the range of 7.8−30.0 min (Table 1; 2−10, 12, 14, 18, 20−22, 28, 29, 33, 49, 50, and 52), were characterized from SST. Amongst them, compounds paeoniflorin sulfonate (**9**), isomaltpaeoniflorin (**10**), albiflorin (**12**), paeoniflorin (**14**), galloylpaeoniflorin (**20**), lactiflorin (**29**), benzoylpaeoniflorin (**50**), and paeonivayin (**52**) (Table 1), were identified by comparison with reference compounds. Other MTG components were tentatively characterized by integrated analysis of their (±) ESI-MS^n data. The characterization of oxypaeoniflorin (compound 6: t_R 9.1 min) was illustrated. Predominant deprotonated and protonated precursors (*m/z* 495/497) were observed for this component, indicating additional 16 Da larger than paeoniflorin (**14**) that had been identified by comparison with the reference compound. CID-MS^2 of the precursor *m/z* 495 yielded abundant product ions at *m/z* 465 ($[M - H - CH_2O]^-$), 375 ($[M - H - 120\ Da]^-$), 333 ($[M - H - Glc]^-$), and 281. The neutral loss of 120 Da together with the MS^3 fragment of *m/z* 281 at *m/z* 137 (base peak) indicated the presence of *p*-hydroxybenzoyl substituent [14, 19]. The positive CID-MS^2 of precursor *m/z* 497 generated the fragments of *m/z* 335 ($[M + H - Glc]^+$) and 197 ($[M + H - Glc - (p\text{-}OH\text{-}BZA)]^+$). These evidences could help characterize compound 6 as oxypaeoniflorin, and its fragmentation pathways are illustrated in Fig. A. Interestingly, we detected a triglycoside (**5**: t_R 8.9 min) and diglycoside (**7**: t_R 9.3 min) of paeoniflorin sulfonate (**9**), which were featured by the successive Glc eliminations yielding a product ion of *m/z* 543 by negative CID. These two components were not reported in precious document regarding MTG characterization of PRA [15].

Galloyl glucoses from SST. Four galloyl glucose components, involving a pentagalloyl glucose (**19**: t_R 15.6 min) and three tetragalloyl glucose isomers (**11**: t_R 11.8 min; 15: t_R 13.2 min; **16**: t_R 13.7 min), were characterized from SST based on the characteristic neutral eliminations of 152 Da (galloyl) and 170 Da (GLA). Compound **19** was identified by comparison with the reference compound. The exact structures of three isomeric tetragalloyl glucoses (**11**, **15**, and **16**) are difficult to be established only by the available MS^n data [15].

Ginsenosides from SST. Despite the low amount of GSL total ginsenosides in the ingredient of SST (accounting for 0.66%), a number of ginsenosides (**55** in total) got characterized from SST, including ginsenosides Rg_1 (**31**), Re (**32**), Rb_1 (**56**), Rc (**62**), Rb_2 (**66**), Rb_3 (**67**), Rd (**70**), F_2 (**79**), and 20(*S*)-Rg_3 (**80**) identified by comparison with the reference compounds. Diagnostic information for characterizing ginsenosides involves characteristic sapogenin ions (*m/z* 459, 475,

and 455 in ESI^- mode; *m/z* 443/425/407 and 459/441/423/405 in ESI^+ mode), and neutrally eliminated masses (162 Da for Glc; 146 Da for Rha, 132 Da for Xyl or Ara). Also, the general retention order, PPT type < PPD type, was useful to identify the sapogenins [24, 26]. These ginsenosides characterized from SST consist of 32 PPT type (**13**, **23**−**27**, **31**, **32**, **34**, **36**, **37**, **39**, **41**, **43**−**48**, **51**, **53**−**55**, **57**−**61**, **63**−**6**5, and **69**), 12 PPD type (**56**, **62**, **66**, **67**, **70**−**72**, **74**−**76**, **79**, and **80**), and 11 with varied sapogenins (**30**, **35**, **38**, **41**, **42**, **68**, **73**, **77**, **78**, **81**, and **82**). We here do not depict the characterization of those unknown ginsenosides, more information can be referred to our previous reports regarding the comprehensive ginsenoside characterization [22−24, 26−29]. New findings in the present study were from the positive ISCID of ginsenosides, providing complementary information for primary characterization of the sapogenin moieties based on the concomitant H_2O-elimination resulting protonated product ion species. For instance, the full-scan spectra at 23.0 min (40: [OH + PPT] − Glc) displayed rich ions at 475, 457, 439, and 421, together with the sodium-adduct precursor at *m/z* 677. These sapogenin ions could suggest a hydroxyl-PPT sapogenin (M.F.: 492), in accordance with the sapogenin ion observed in negative CID at *m/z* 491. In contrast to our previous research focusing on the ginsenosides of GSL [24], no OA type or malonylginsenosides were detected and identified from SST, which may attribute to their low content and the preparation technique of total ginsenosides of GSL.

Table 1 Chemical components identified from SST by HPLC/DAD/(±) ESI-MS^n

No.	t_R/min	UV	Identification	M. F.	$[M-H]^-$/$[M+HCOO]^-$/$[M+H]^+$/$[M+Na]^+$/$[M+NH_4]^+$	Source
1[a]	5.3	226, 268	gallic acid	$C_7H_6O_5$	169/(−)/(−)/(−)/(−)	PRA
2	7.8	216, 260	oxypaeoniflorin sulfonate or isomer	$C_{23}H_{28}O_{14}S$	559/(−)/(−)/(−)/(−)	PRA
3	8.5	222, 278	mudanpioside E sulfonate or isomer	$C_{24}H_{30}O_{15}S$	589/(−)/(−)/(−)/(−)	PRA
4	8.7	222, 282	6'-*O*-galloyl desbenzoylpaeoniflorin	$C_{23}H_{28}O_{14}$	527/(−)/(−)/(−)/(−)	PRA
5	8.9	226, 272	paeoniflorin sulfonate-Glc-Glc-Glc	$C_{41}H_{58}O_{28}S$	1029/(−)/(−)/(−)/(−)	PRA
6	9.1	224, 262	oxypaeoniflorin	$C_{23}H_{28}O_{12}$	495/(−)/497/(−)/(−)	PRA
7	9.3	232, 276	paeoniflorin sulfonate-Glc-Glc	$C_{35}H_{48}O_{23}S$	867/(−)/(−)/(−)/886	PRA
8	9.7	232, 276	isomaltopaeoniflorin sulfonate	$C_{29}H_{38}O_{18}S$	705/(−)/(−)/(−)/724	PRA
9[a]	10.7	234	paeoniflorin sulfonate	$C_{23}H_{28}O_{13}S$	543/(−)/(−)/(−)/562	PRA; U
10[a]	11.6	234	isomaltpaeoniflorin	$C_{29}H_{38}O_{16}$	641/687/(–)/665/660	PRA
11	11.8	226, 282	tetragalloyl glucose	$C_{34}H_{28}O_{22}$	787/(−)/(−)/(−)/806	PRA
12[a]	12.1	232	albiflorin	$C_{23}H_{28}O_{11}$	479/525/481/503/498	PRA; U
13	12.7	n.a.	20-*O*-Glc-ginsenoside Rf	$C_{48}H_{82}O_{19}$	961/1007/(–)/985/(–)	GSL
14[a]	12.9	232	paeoniflorin	$C_{23}H_{28}O_{11}$	479/525/481/503/498	PRA; U
15	13.2	226, 280	tetragalloyl glucose	$C_{34}H_{28}O_{22}$	787/(−)/(−)/(−)/806	PRA
16	13.7	228, 280	tetragalloyl glucose	$C_{34}H_{28}O_{22}$	787/(−)/(−)/(−)/806	PRA
17[a]	14.7	228, 270	ethyl gallate	$C_9H_{10}O_5$	197/(−)/(−)/(−)/(–)	PRA; U
18	15.0	254, 368	galloylpaeoniflorin sulfonate	$C_{30}H_{32}O_{17}S$	695/(−)/(−)/(−)/(−)	PRA
19[a]	15.6	228, 280	pentagalloyl glucose	$C_{41}H_{32}O_{26}$	939/(−)/(−)/963/958	PRA
20[a]	16.0	224, 274	galloylpaeoniflorin	$C_{30}H_{32}O_{15}$	631/(−)/633/655/650	PRA
21	17.1	232, 280	isomer of galloylpaeoniflorin	$C_{30}H_{32}O_{15}$	631/(−)/633/655/650	PRA
22	17.7	228, 280	isomer of galloylpaeoniflorin	$C_{30}H_{32}O_{15}$	631/(−)/633/655/650	PRA
23	18.8	n.a.	PPT-Glc-Glc-Xyl	$C_{47}H_{80}O_{18}$	931/977/(−)/(−)/(−)	GSL
24	19.4	n.a.	ginsenoside Rh18 or isomer	$C_{48}H_{80}O_{18}$	943/989/(−)/967/(−)	GSL; U
25	19.6	n.a.	notoginsenoside R_1 or isomer	$C_{47}H_{80}O_{18}$	931/977/(−)/955/(−)	GSL
26	20.0	n.a.	PPT-Glc-Glc-Xyl	$C_{47}H_{80}O_{18}$	931/977/(−)/955/(−)	GSL
27	20.2	n.a.	ginsenoside Rh18 or isomer	$C_{48}H_{80}O_{18}$	943/989/(−)/(−)/(−)	GSL; U
28	21.0	276	3', 6'-di-*O*-galloylpaeoniflorin or isomer	$C_{37}H_{36}O_{19}$	783/(−)/(−)/(−)/802	PRA
29[a]	21.2	234	lactiflorin	$C_{23}H_{26}O_{10}$	461/507/(−)/(−)/(−)	PRA
30	21.2	n.a.	(PPT+H_2O)-Glc-Glc-Glc	$C_{48}H_{84}O_{20}$	979/1025/(−)/1003/(−)	GSL
31[a]	21.4	n.a.	ginsenoside Rg_1	$C_{42}H_{72}O_{14}$	799/845/(−)/823/(−)	GSL; U
32[a]	21.4	n.a.	ginsenoside Re	$C_{48}H_{82}O_{18}$	945/991/947/969/(−)	GSL; U; P
33	21.6	276	3', 6'-di-*O*-galloylpaeoniflorin or isomer	$C_{37}H_{36}O_{19}$	783/(−)/(−)/(−)/802	PRA
34	21.7	n.a.	notoginsenoside Rw2 or isomer	$C_{41}H_{70}O_{14}$	785/831/(−)/809/(−)	GSL
35	22.0	n.a.	(PPT+H_2O)-Glc-Glc-Glc	$C_{48}H_{84}O_{20}$	979/1025/(−)/1003/(−)	GSL
36	22.1	n.a.	isomer of Rh18	$C_{48}H_{80}O_{18}$	943/989/(−)/967/(−)	GSL
37	22.4	n.a.	notoginsenoside Rw2 or isomer	$C_{41}H_{70}O_{14}$	785/831/787/809/(−)	GSL
38	22.6	n.a.	(OH + PPT)-Glc	$C_{36}H_{62}O_{10}$	653/699/(−)/677/(−)	GSL

Continued

No.	t_R(min)	UV	Identification	M. F.	$[M-H]^-/[M+HCOO]^-/[M+H]^+/[M+Na]^+/[M+NH_4]^+$	Source
39	22.8	n.a.	floralginsenoside P or isomer	$C_{53}H_{90}O_{23}$	1093/1139/(−)/(−)/(−)	GSL
40	23.0	n.a.	(OH + PPT)-Glc	$C_{36}H_{62}O_{10}$	653/699/(−)/677/(−)	GSL
41	23.2	n.a.	floralginsenoside P or isomer	$C_{53}H_{90}O_{23}$	1093/1139/(−)/(−)/(−)	GSL
42	23.2	n.a.	notoginsenoside G or isomer	$C_{48}H_{80}O_{19}$	959/1005/(−)/963/(−)	GSL
43	23.4	n.a.	floralginsenoside P or isomer	$C_{53}H_{90}O_{23}$	1093/1139/1005/1117/(−)	GSL
44	23.7	n.a.	PPT-Rha-Rha	$C_{42}H_{72}O_{13}$	767/813/(−)/791/(−)	GSL
45	23.9	n.a.	isomer of floralginsenoside P	$C_{53}H_{90}O_{23}$	1093/1139/(−)/1117/(−)	GSL
46	24.4	n.a.	notoginsenoside R3 or isomer	$C_{48}H_{82}O_{19}$	961/1007/(−)/985/(−)	GSL
47	25.3	n.a.	notoginsenoside R3 or isomer	$C_{48}H_{82}O_{19}$	961/1007/(−)/985/(−)	GSL
48	25.5	n.a.	notoginsenoside R3 or isomer	$C_{48}H_{82}O_{19}$	961/1007/(−)/985/(−)	GSL; U; P
49	25.5	236, 276	benzoylpaeoniflorin sulfonate	$C_{30}H_{32}O_{14}S$	647/(−)/(−)/(−)/666	PRA
50 [a]	28.8	232	benzoylpaeoniflorin	$C_{30}H_{32}O_{12}$	583/629/(−)/607/602	PRA
51	29.7	n.a.	isomer of ginsenoside Rf	$C_{42}H_{72}O_{14}$	799/845/801/823/(−)	GSL
52 [a]	30.0	232	paeonivayin	$C_{30}H_{32}O_{12}$	583/629/585/607/602	PRA
53	30.7	n.a.	ginsenoside Rf	$C_{42}H_{72}O_{14}$	799/845/(−)/823/(−)	GSL
54	31.1	n.a.	notoginsenoside R_1 isomer	$C_{47}H_{80}O_{18}$	931/977/(−)/955/(−)	GSL
55	32.4	n.a.	notoginsenoside R_2	$C_{41}H_{70}O_{13}$	769/815/771/793/(−)	GSL; U
56 [a]	32.5	n.a.	ginsenoside Rb_1	$C_{54}H_{92}O_{23}$	1107/1153/1109/1131/(−)	GSL
57	32.7	n.a.	isomer of notoginsenoside R1	$C_{47}H_{80}O_{18}$	931/977/(−)/955/(−)	GSL
58	33.6	n.a.	ginsenoside F3/F5 or isomer	$C_{41}H_{70}O_{13}$	769/815/771/793/(−)	GSL; U
59	34.2	n.a.	ginsenoside F3/F5 or isomer	$C_{41}H_{70}O_{13}$	769/815/771/793/(−)	GSL
60	33.8	n.a.	20(*S*)-ginsenoside Rg_2	$C_{42}H_{72}O_{13}$	783/829/(−)/(−)/(−)	GSL; U
61	34.5	n.a.	20(*R*)-ginsenoside Rg_2	$C_{42}H_{72}O_{13}$	783/829/(−)/(−)/(−)	GSL; U
62 [a]	34.6	n.a.	ginsenoside Rc	$C_{53}H_{90}O_{22}$	1077/1123/1079/1101/(−)	GSL; U; P
63	34.7	n.a.	ginsenoside Rh_1	$C_{36}H_{62}O_9$	637/683/(−)/661(−)	GSL
64	34.8	n.a.	isomer of ginsenoside Rf	$C_{42}H_{72}O_{14}$	799/845/(−)/823/(−)	GSL
65	36.4	n.a.	isomer of ginsenoside Rf	$C_{42}H_{72}O_{14}$	799/845/(−)/823/(−)	GSL
66 [a]	36.8	n.a.	ginsenoside Rb_2	$C_{53}H_{90}O_{22}$	1077/1123/1079/1101/(−)	GSL; U; P
67 [a]	37.5	n.a.	ginsenoside Rb_3	$C_{53}H_{90}O_{22}$	1077/1123/(−)/1101/(−)	GSL; U; P
68	37.8	n.a.	(PPT-2H)-Glc-Xyl	$C_{41}H_{68}O_{13}$	767/813/(−)/791/(−)	GSL
69	40.4	n.a.	ginsenoside F1	$C_{36}H_{62}O_9$	637/683/639/661/(−)	GSL; U
70 [a]	42.1	n.a.	ginsenoside Rd	$C_{48}H_{82}O_{18}$	945/991/(−)/969/(−)	GSL; U; P
71	43.1	n.a.	notoginsenoside U or isomer	$C_{42}H_{72}O_{14}$	799/845/(−)/823/(−)	GSL
72	46.2	n.a.	notoginsenoside K	$C_{48}H_{82}O_{18}$	945/991/947/969/(−)	GSL
73	47.4	n.a.	ginsenoside Rh7 or isomer	$C_{36}H_{60}O_9$	635/681/637/659/(−)	GSL
74	49.2	n.a.	isomer of ginsenoside Rd	$C_{48}H_{82}O_{18}$	945/991/(−)/969/(−)	GSL
75	49.7	n.a.	vinaginsenoside R16 or isomer	$C_{47}H_{80}O_{17}$	915/961/(−)/(−)/(−)	GSL; U
76	51.3	n.a.	vinaginsenoside R16 or isomer	$C_{47}H_{80}O_{17}$	915/961/(−)/(−)/(−)	GSL; U; P
77	53.2	n.a.	ginsenoside Rg6 or isomer	$C_{42}H_{70}O_{12}$	765/811/(−)/(−)/(−)	GSL; U
78	54.0	n.a.	ginsenoside Rg6 or isomer	$C_{42}H_{70}O_{12}$	765/811/767/(−)/(−)	GSL; U
79 [a]	54.4	n.a.	ginsenoside F2	$C_{42}H_{72}O_{13}$	783/829/(−)/807/(−)	GSL; U
80 [a]	55.5	n.a.	20(*S*)-ginsenoside Rg3	$C_{42}H_{72}O_{13}$	783/829/(−)/807/(−)	GSL; U
81	57.6	n.a.	ginsenoside Rk1 or isomer	$C_{42}H_{70}O_{12}$	765/811/(−)/(−)/(−)	GSL
82	57.8	n.a.	ginsenoside Rk1 or isomer	$C_{42}H_{70}O_{12}$	765/811/(−)/(−)/(−)	GSL

n.a.: not available;

[a]: identified by comparison with reference compounds

Compounds **1** (t_R: 5.3 min) and **17** (t_R: 14.7 min), as two phenol components, were identified from SST by comparison with the reference compounds in respect of retention time and ESI-MS^n information.

Identification of the components in plasma and urine samples after oral administration of SST in rats

To detect and characterize the absorbed components in rats, a high dosage of SST extract (equal to 4 g SST/kg body weight) was given to rats by oral administration. The blood samples at four different time points (0.5, 1.5, 4, and 12 h) and urine samples from 0 to 24 h were collected for analysis. As a result, seven components were identified from plasma and 24 from urine based on their retention behavior, UV spectra, MS^n data, and comparison with the chemical list of SST (Table 1). It was noted, all these components characterized from rat plasma and urine were prototypes, without phases I/II metabolites or other transformed ingredients.

The components of SST that were absorbed into blood, we detected in the present study, were all ginsenosides, including ginsenoside Re (32), notoginsenoside R_3 or isomer (48), ginsenosides Rc (62), Rb_2 (66), Rb_3 (67), Rd (70), and vinaginsenoside R_{16} or isomer (76). Among them, two were PPT type, and the other five belonged to PPD type.

The components detected in rat urine were composed by three MTGs (9: paeoniflorin sulfonate; 12: albiflorin; 14: paeoniflorin) and ethyl gallate (17) from PRA, and 20 ginsenosides (24, 27, 31, 32, 48, 55, 58, 60−62, 66, 67, 69, 70, and 75−80) from GSL.

Despite we have carefully checked the data of the rat plasma and urine samples by extracted ion chromatograms (EIC) of those reported in literature [33, 34], only the prototypes of MTGs were observed. In addition, the difficulty in detecting ginsenoside metabolites in rat plasma and urine was consistent with a previous report [35], which could be attributed to their transformation and degradation by gut microorganisms after oral administration.

Conclusion

An HPLC/DAD/ESI-MS^n approach was established, which enabled the simultaneous characterization of SST components and those absorbed by rats. By use of an Eclipse XDB C18 column and acetonitrile/0.1% formic acid as the mobile phase, well resolution of the multicomponents in SST was achievable. Integrated analyses of the MS^n data obtained by both negative and positive CIDs offered abundant, and more importantly, complementary structural information for their identification. In light of these efforts, a total of 82 components, including 21 MTGs, four galloyl glucoses, two phenols from PRA, and 55 ginsenosides from GSL, were identified or tentatively characterized from SST. Amongst them, seven and 24 compounds were detected from the plasma and urine samples of rats, respectively, after oral administration of an SST extract. All these components identified from rat plasma and urine were the prototype compounds. To the best of our knowledge, this was the first report unveiling the chemical complexity of SST and its potential therapeutic basis, which would beneficial to investigating its curative effects on CHD and quality control.

References

[1] Yang WZ, Zhang YB, Wu WY, *et al*. Approaches to establish Q-markers for the quality standards of traditional Chinese medicines [J]. *Acta Pharm Sin B*, 2017, **7**(4): 439-446.

[2] Wolfender JL, Marti G, Thomas A, *et al*. Current approaches and challenges for the metabolite profiling of complex natural extracts [J]. *J Chromatogr A*, 2015, **1382**: 136-164.

[3] Ma FX, Xue PF, Wang YY, *et al*. Research progress of serum pharmacochemistry of traditional Chinese medicine [J]. *Chin J Chin Mater Med*, 2017, **42**(7): 1265-1270.

[4] Ganzera M, Sturm S. Recent advances on HPLC/MS in medicinal plant analysis-An update covering 2011−2016 [J]. *J Pharm Biomed Anal*, 2018, **147**: 211-233.

[5] Wei WF, Chen HC, Liu Y, *et al*. Preliminary study on serum pharmacochemistry of leaves of *Acanthopanax senticosus* based on UPLC-Q-TOF-MS [J]. *Chin Tradit Herbal Drugs*, 2017, **48**(7): 1306-1313.

[6] Lu JJ, Hu XW, Li P, *et al*. Global identification of chemical constituents and rat metabolites of Si-Miao-Wan by liquid chromatography-electrospray ionization/quadrupole time-of-flight mass spectrometry [J]. *Chin J Nat Med*, 2017, **15**(7): 550-560.

[7] Wang DM, Xu YF, Chen Z, *et al*. UPLC/Q-TOF-MS analysis of iridoid glycosides and metabolites in rat plasma after oral administration of *Paederia scandens* extracts [J]. *Chin J Nat Med*, 2015, **13**(3): 215-221.

[8] Miao WJ, Wang Q, Bo T, *et al*. Rapid characterization of chemical constituents and rats metabolites of the traditional Chinese patent medicine Gegen-Qinlian-Wan by UHPLC/DAD/qTOF-MS [J]. *J Pharm Biomed Anal*, 2013, **72**: 99-108.

[9] Wang J, He QY, Zhang YL. Effect of Shenshao Tablet on the quality of life for coronary heart disease patients with stable angina pectoris [J]. *Chin J Integr Med*, 2009, **15**(5): 328-332.

[10] Chen S, Han Q, Liu WJ, *et al*. Shenshao Tablet/capsules in the treatment of coronary heart disease: a meta-analysis of clinical randomized controlled trials [J]. *Chin J Integr Med Cardio*, 2017, **15**(17): 2089-2094.

[11] Commission of National Pharmacopoeia. *Chinese Pharmacopoeia (part I)* [S]. Chinese Medical Science and Technology Press, Beijing. 2015: 1126

[12] Cui H, Zhu JQ, Feng QF, *et al*. Advances in researches of the chemical constituents and biological activities of the traditional Chinese medicine Paeoniae Radix Alba [J]. *Strait Pharm J*, 2017, **29**(9): 1-5.

[13] Wu SH, Wu DG, Chen YW. Chemical constituents and bioactivities of plants from the genus *Paeonia* [J]. *Chem Biodivers*, 2010, **7**: 90-104.

[14] Liu EH, Qi LW, Li B, *et al*. High-speed separation and characterization of major constituents in Radix Paeoniae Rubra by fast high-performance liquid chromatography coupled with diode-array detection and time-of-flight mass spectrometry [J]. *Rapid Commun Mass Spectrom*, 2009, **23**(1): 119-130.

[15] Li SL, Song JZ, Choi FFK, *et al*. Chemical profiling of Radix Paeoniae evaluated by ultra-performance liquid chromatogra-

phy/photo-diode-array/quadrupole time-of-flight mass spectrometry [J]. *J Pharm Biomed Anal*, 2009, **49**(2): 253-266.

[16] Dong HJ, Liu ZQ, Song FR, *et al*. Structural analysis of monoterpene glycosides extracted from *Paeonia lactiflora* Pall. using electrospray ionization Fourier transform ion cyclotron resonance mass spectrometry and high-performance liquid chromatography/electrospray ionization tandem mass spectrometry [J]. *Rapid Commun Mass Spectrom*, 2007, **21**(19): 3193-3199.

[17] Cao J, Qiao X, Ji S, *et al*. Insights into the neutral loss of 30 Da of *Paeonia* monoterpene glycosides in electrospray ionization tandem mass spectrometry and the rapid screening of monoterpene glycosides by LC/MS/MS [J]. *J Chin Pharm Sci*, 2016, **25**(1): 37-45.

[18] Li JH, Kuang G, Chen XH, *et al*. Identification of chemical composition of leaves and flowers from *Paeonia rockii* by UHPLC-Q-Exactive Orbitrap HRMS [J]. *Molecules*, 2016, **21**(7): 947.

[19] Cao G, Li QL, Cai H, *et al*. Investigation of the chemical changes from crude and processed Paeoniae Radix Alba-Atractylodis Macrocephalae Rhizoma Herbal pair extracts by using Q Exactive high-performance benchtop quadrupole-Orbitrap LC-MS/MS [J]. *Evid Based Complement Alternat Med,* 2014: 170959.

[20] Li FL. Research progress of pharmacology effects about ginsenosides from stems and leaves of *Panax ginseng* [J]. *Guizhou Agric Sci*, 2013, **41**(2): 54-57.

[21] Lee JW, Choi BR, Kim YC, *et al*. Comprehensive profiling and quantification of ginsenosides in the root, stem, leaf, and berry of *Panax ginseng* by UPLC-QTOF/MS [J]. *Molecules*, 2017, **22**: 2147.

[22] Yang WZ, Hu Y, Wu WY, *et al*. Saponins in the genus *Panax* L. (Araliaceae): A systematic review of their chemical diversity [J]. *Phytochemistry*, 2014, **106**: 7-24.

[23] Qiu S, Yang WZ, Yao CL, *et al*. Nontargeted metabolomic analysis and "commercial-homophyletic" comparison-induced biomarkers verification for the systematic chemical differentiation of five different parts of *Panax ginseng* [J]. *J Chromatogr A*, 2016, **1453**: 78-87.

[24] Qiu S, Yang WZ, Shi XJ, *et al*. A green protocol for efficient discovery of novel natural compounds: characterization of new ginsenosides from the stems and leaves of *Panax ginseng* as a case study [J]. *Anal Chim Acta*, 2015, **893**: 65-76.

[25] Xu SJ, Yang L, Zeng X, *et al*. Characterization of compounds in the Chinese herbal drug Mu-Dan-Pi by liquid chromatography coupled to electrospray ionization mass spectrometry [J]. *Rapid Commun Mass Spectrom*, 2006, **20**(22): 3275-3288.

[26] Yang WZ, Ye M, Qiao X, *et al*. A strategy for efficient discovery of new natural compounds by integrating orthogonal column chromatography and liquid chromatography/mass spectrometry analysis: its application in *Panax ginseng*, *Panax quinquefolium* and *Panax notoginseng* to characterize 437 potential new ginsenosides [J]. *Anal Chim Acta*, 2012, **739**: 56-66.

[27] Yang WZ, Qiao X, Li K, *et al*. Identification and differentiation of *Panax ginseng*, *Panax quinquefolium*, and *Panax notoginseng* by monitoring multiple diagnostic chemical markers [J]. *Acta Pharm Sin B*, 2016, **6**(6): 568-575.

[28] Yang WZ, Bo T, Ji S, *et al*. Rapid chemical profiling of saponins in the flower buds of *Panax notoginseng* by integrating MCI gel column chromatography and liquid chromatography/mass spectrometry analysis [J]. *Food Chem*, 2013, **139**(1−4): 762-769.

[29] Yang WZ, Zhang JX, Yao CL, *et al*. Method development and application of offline two-dimensional liquid chromatography/quadrupole time-of-flight mass spectrometry-fast data directed analysis for comprehensive characterization of the saponins from Xueshuantong Injection [J]. *J Pharm Biomed Anal*, 2016, **128**: 322-332.

[30] Stavrianidi A, Rodin I, Braun A, *et al*. The use of linear ion trap for qualitative analysis of phytochemicals in Korean ginseng tea [J]. *Biomed Chromatogr*, 2013, **27**(6): 765-774.

[31] Qi LW, Wang HY, Zhang H, *et al*. Diagnostic ion filtering to characterize ginseng saponins by rapid liquid chromatography with time-of-flight mass spectrometry [J]. *J Chromatogr A*, 2012, **1230**: 93-99.

[32] Chan TWD, But PPH, Cheng SW, *et al*. Differentiation and authentication of *Panax ginseng*, *Panax quinquefolius*, and ginseng products by using HPLC/MS [J]. *Anal Chem*, 2000, **72**(6): 1281-1287.

[33] Cao WL, Wang XG, Li HJ, *et al*. Studies on metabolism of total glucosides of paeony from Paeoniae Radix Alba in rats by UPLC-Q-TOF-MS/MS [J]. *Biomed Chromatogr*, 2015, **29**(11): 1769-1779.

[34] Liang J, Xu F, Zhang YZ, *et al*. The profiling and identification of the absorbed constituents and metabolites of Paeoniae Radix Rubra decoction in rat plasma and urine by the HPLC-DAD-ESI-IT-TOF-MS^n technique: a novel strategy for the systematic screening and identification of absorbed constituents and metabolites from traditional Chinese medicines [J]. *J Pharm Biomed Anal*, 2013, **83**: 108-121.

[35] Rong YY, Feng SX, Wu CW, *et al*. LC-high-resolution-MS/MS analysis of chemical compounds in rat plasma after oral administration of Nao-Mai-Tong and its individual herbs [J]. *Biomed Chromatogr*, 2017, **31**(7): e3920.

Cite this article as: MIAO Wen-Juan, HU Ying, JIA Li, ZHANG Chun-Xia, YANG Wen-Zhi, ZHANG Ping, GUO De-An. Profiling and identification of chemical components of Shenshao Tablet and its absorbed components in rats by comprehensive HPLC/DAD/ESI-MS^n analysis [J]. *Chin J Nat Med*, 2018, **16**(10): 791-800.

Prof. GUO De-An, working as a chair professor in Shanghai Institute of Materia Medica, Chinese Academy of Sciences, director of National Engineering Laboratory for TCM Standardization Technology, director of Shanghai Research Center for TCM Modernization. He focused his research on the modernization of traditional Chinese medicine for more than 30 years. He is the first Chinese scientist to elaborate TCM standards for USP and EP. He published over 420 SCI papers, and 25 authorized patents.